

Multiphonon processes in resonant scattering and exciton luminescence of crystals

A. A. Klyuchikhin, S. A. Permogorov, and A. N. Reznitskiĭ

A. F. Ioffe Physico-technical Institute, USSR Academy of Sciences

(Submitted May 20, 1976)

Zh. Eksp. Teor. Fiz. 71, 2230-2251 (December 1976)

We investigated experimentally the spectra of multiphonon resonant Raman scattering in CdS crystals and of exciton-phonon luminescence in CdS and CdSe crystals. Raman scattering and luminescence of free excitons with excitation up to four LO phonons have been investigated for the first time. The intensity distribution in the observed spectra is analyzed. The temperature dependence of the shape and the intensity of the exciton-phonon luminescence lines is investigated. It is established that the cross sections of odd order depend on the value of the wave vector transferred to the phonon system. It is shown that the predominant part in resonant multiphonon scattering is played by long-wave phonons with wave vectors on the order of the reciprocal Bohr radius of the exciton. A theory of multiphonon resonant Raman scattering by LO phonons is developed, in which free electron-hole pairs as well as states of the discrete and continuous spectra of the free excitons are treated as intermediate states. A comparison of the theory with experiment shows that the theory accounts well for the main experimental results both below the threshold and in the region of intrinsic absorption. It is shown that to explain the scattering processes below the absorption edge, as well as the luminescence processes, it is important in principle to take into account the excited states of the exciton.

PACS numbers: 78.30.Gt, 78.60.-b, 71.80.+j

I. INTRODUCTION

An investigation of resonant scattering of light near the intrinsic absorption edge makes it possible to obtain extensive information on the nature and mechanisms of electron-phonon interaction. The high intensity of the resonant-scattering spectra adds greatly to the experimental possibilities and makes it possible in principle to observe new phenomena. One such phenomenon is multiphonon scattering of light. The appearance of higher-order processes is a sufficiently general property of resonant scattering. In semiconductors, multiphonon scattering of light was observed experimentally following excitation in the region of the intrinsic absorption.^[1,2] Multiphonon scattering of light by crystals was considered theoretically in a number of papers.^[3,4,5] There is at present, however, no sufficiently clear picture of this phenomenon.

In this paper we report an experimental and theoretical investigation of multiphonon resonant Raman scattering and of exciton-phonon luminescence with excitation of LO phonons in CdS and CdSe crystals. With the crystals excited below the intrinsic absorption edge, we succeeded in observing for the first time Raman scattering processes with excitation up to four LO phonons. In the same crystals, we observed multiphonon luminescence of the free excitons and investigated the temperature dependence of the shape and intensity of the exciton-phonon bands of third and fourth order. It follows from our results that the principal regularities of the observed phenomena can be explained in the framework of a theoretical model in which free excitons are treated as intermediate states. The interaction of the excitons with phonons is treated by perturbation theory via the mechanism of the intraband Fröhlich electron-phonon scattering. Taking into account the rather general character of the employed assumptions, one can hope that our main conclusions are valid for an extensive

class of polar semiconductors with a clearly pronounced exciton structure of the intrinsic absorption edge.

Our study shows that the multiphonon scattering has essentially different properties in the case of excitation above and below the intrinsic-absorption edge. In the region above the intrinsic-absorption edge, the multiphonon lines of different orders have comparable intensity. The scattering process has in this case the characteristic feature of the luminescence of hot excitons.^[6] In particular, the scattering intensity depends on the lifetime of the intermediate states and is subject to quenching. The main intermediate scattering states are hot excitons with principal quantum number $n = 1$.

Multiphonon scattering below the intrinsic-absorption edge and exciton-phonon luminescence are characterized by a rapid decrease of the intensity with increasing number of excited phonons. The even and odd processes have essentially different dependences of the cross section on the wave vector $|\mathbf{k} - \mathbf{k}'|$ transferred to the phonon system. Whereas the cross section of a multiphonon process of even order is practically independent of the wave vector $|\mathbf{k} - \mathbf{k}'|$, the cross section of a process of odd order always contains a part proportional to $|\mathbf{k} - \mathbf{k}'|^2$. This difference is due to the different character of the sequence of the intermediate states. It has been established that in the analysis of the scattering below the edge and of exciton-phonon luminescence, an important role is played by allowance for the exciton states with $n \geq 2$ as intermediate states. Allowance for these states leads to a characteristic phenomenon of size-dependent resonance in first-order scattering.^[7,8] The cross section of the multiphonon scattering above and below the intrinsic-absorption edge is also a significantly different frequency dependence. The results of the theoretical analysis and of the numerical estimates are in good agreement with experiment.

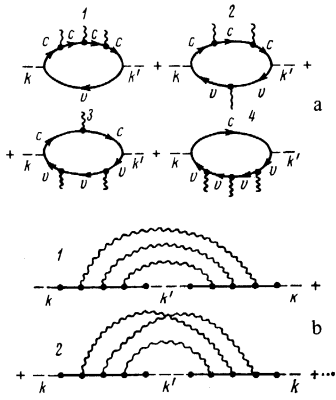


FIG. 1. a) Resonant topologically inequivalent diagrams of three-phonon scattering amplitude. Solid lines—electron Green's functions, dashed lines—photons, wavy lines—phonons. b) Diagrams of the "forward" scattering amplitude for a photon with a wave vector \mathbf{k} and frequency ω . Solid lines—exciton Green's function. The jump of this amplitude with respect to the frequency ω gives the cross section for the third-order scattering of the photon (\mathbf{k}, ω).

II. THEORY

The microscopic mechanism of Raman scattering with emission of l phonons can be described by the following sequence of processes: (a) virtual absorption of the incident photon of frequency ω ; (b) transition of the system from the state produced after the absorption of the incident photon into other states with successive¹⁾ emission of l phonons; (c) emission of the scattered photon with frequency ω' . For dielectrics with completely filled valence bands and empty conduction bands, processes (a) and (c) consist of virtual production and annihilation of an electron-hole pair or of an exciton; we confine ourselves to the case when both processes are allowed in the dipole approximation. We consider a situation typical of resonant scattering, when ω and ω' are close to the edge of the band ε_g . This allows us to separate the two-band terms of the amplitude, which exhibit the most resonant behavior. The scattering amplitude was calculated by a diagram technique.^[9]

Excitonless case

1. When the intermediate states are free electron-hole pairs, the sum of all the resonant topologically non-equivalent diagrams for the amplitude of order l can be represented in the form

$$A_l^{\alpha\beta}(\omega) = \frac{(2\pi)^2 e^2}{(\omega\omega')^{1/2}} \frac{v_{vc}^\alpha v_{cv}^\beta}{\hbar^{l+1} v_0^2} \frac{\delta(\mathbf{k} - \mathbf{k}' - \sum_{i=1}^l \mathbf{q}_i) \delta(\omega - \omega' - \sum_{i=1}^l \Omega_{q_i})}{\omega - \Omega_{p_0}^{cv} - \hbar k^2/2M} \times \prod_{m=1}^l \frac{[\Xi_{cc}(q_m) e^{iq_m^c \mathbf{r}} - \Xi_{vv}(q_m) e^{-iq_m^v \mathbf{r}}] p_{m-1} p_m}{\omega_m - \Omega_{p_m}^{cv} - \hbar Q_m^2/2M}. \quad (1)$$

Here v_0 is the volume of the unit cell, \mathbf{v}_{vc} is the interband matrix element of the electron velocity operator; \mathbf{k} and \mathbf{k}' are the wave vectors of the incident and scattered light; Ω_{q_i} is the frequency of a phonon with wave vector q_i ; $q_i^{\alpha v} = q_i \mu / m_{c,v}$; $\mu^{-1} = m_c^{-1} + m_v^{-1}$; $M = m_c + m_v$; $\Omega_p^{cv} = \varepsilon_p^c - \varepsilon_p^v + \varepsilon_g$; $\omega_m = \omega - \sum_{i=1}^m \Omega_{q_i}$; $Q_m = \mathbf{k} - \sum_{i=1}^m \mathbf{q}_i$; $\Xi_{cc}(q)$ and $\Xi_{vv}(q)$ are the intraband matrix elements of the elec-

tron-phonon interaction. The symbol $[\dots]_{p_{m-1} p_m}$ denotes the matrix elements of the operator in the bracket with respect to the plane waves $V^{-1/2} \exp(i\mathbf{p}_m \mathbf{r})$ and $V^{-1/2} \times \exp(-i\mathbf{p}_{m-1} \mathbf{r})$, which reduces to an intermediate momentum-conservation law

$$(2\pi)^3 / v_0 [\delta(\mathbf{p}_m - \mathbf{p}_{m-1} + \mathbf{q}_m^c) - \delta(\mathbf{p}_m - \mathbf{p}_{m-1} + \mathbf{q}_m^v)].$$

Integration with respect to the $(l+1)$ variables p_0, p_1, \dots, p_l is left out of expression (1) but is implied.

For LO phonons, the intraband matrix elements of the electron-phonon interaction satisfy the condition

$$\Xi_{cc}(q) = \Xi_{vv}(q) = (qd)^{-1} \Xi_{LO}; \quad \Xi_{LO} = \left[\frac{2\pi e^2}{d} \hbar \Omega_{LO} \left(\frac{1}{\varepsilon_\infty} - \frac{1}{\varepsilon_0} \right) \right]^{1/2}, \quad (2)$$

where d is the lattice constant. We confine ourselves below to the case of scattering by LO phonons. Out of the total number $(l+1)$ integrations with respect to the variables \mathbf{p}_i in (1), l integrations are carried out with the aid of intermediate conservation laws in general form.

2. We consider the asymptotic behavior of the amplitudes of the multiphonon processes in different limiting cases and the behavior of the cross sections near the intrinsic-absorption threshold.

Expanding the product in (1), we obtain 2^l terms that differ from one another in the denominators, on account of the different intermediate momentum conservation laws. Two of these terms differ from the remainder in that they contain one less q_i -dependent denominator than the others. These two terms correspond to two diagrams (Fig. 1) containing all l phonon ends on the upper or lower lines of the electron loop. Their contributions to (1) decrease more slowly than the rest with increasing q_i , and they determine the asymptotic form of the amplitude in the region of large q_i . The values of q_i starting with which the amplitude decreases are given by the relation

$$q_i \approx q_0 = (2\mu/\hbar)^{1/2} [|\varepsilon_g - \omega|^{1/2} + |\varepsilon_g - \omega'|^{1/2}], \quad (3)$$

and in the limit $q_i \gg q_0$ the amplitude is

$$A_l^{\alpha\beta}(\omega) \sim \prod_{i=1}^l \frac{q_p}{q_i} \prod_{m=1}^{l-1} \left(\sum_{k=1}^m \frac{q_k^2}{q_p^2} \right)^{-1}, \quad (4)$$

where $q_p = (2\mu\Omega_{LO}/\hbar)^{1/2}$. The rapid decrease of the amplitude at $q_i \gg q_0$ causes the main contribution to the cross section to be made by the region $0 < q_i \lesssim q_0$ of phonon wave vectors that are small in comparison with the reciprocal lattice constant.

Expanding (1) in a series in q_i at $q_i \ll q_0$ and retaining the minimal powers, we obtain for the amplitudes of the even and odd orders respectively

$$A_l^{\alpha\beta}(\omega) \sim \frac{(p_0 q_1)(p_0 q_2) \dots (p_0 q_l)}{|q_1 q_2 \dots q_l| q_p^l} + O(q^2), \quad (5a)$$

$$A_l^{\alpha\beta}(\omega) \sim \mathcal{A} \frac{(p_0 q_1)(p_0 q_2) \dots (p_0 q_{l-1}) q_l^2}{|q_1 q_2 \dots q_l| q_p^{l+1}} + O(q^2), \quad (5b)$$

where $\mathcal{A} = (m_v - m_c)/2(m_v + m_c)$. The integration with re-

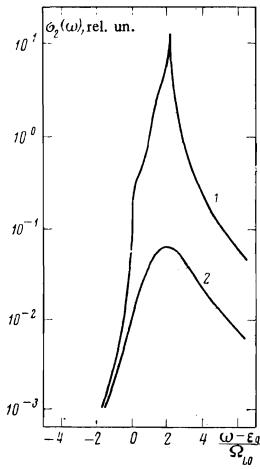


FIG. 2. Frequency dependence of the cross section for scattering with emission of two LO phonons at two values of the electron-damping parameter γ : 1— $\gamma = 0.01 \Omega_{LO}$; 2— $\gamma = \Omega_{LO}$.

spect to the angles between p_0 and q_i determines the difference in the character of the asymptotic forms of the even and odd orders in the region of small q_i , namely, the amplitudes of even order each contain a constant term stemming from allowance for the alternating s and p intermediate states of the electron-hole pairs, whereas the expansion of an odd-order amplitude begins with the first degree of q_i .

We shall show now that as a result of (5b) the amplitudes of odd order turn out to be proportional in the region of small q_i to the difference $|\mathbf{k} - \mathbf{k}'|$ between the wave vectors of the incident and scattered light. Indeed, from (5b) we obtain for the third-order amplitude

$$A_3^{\alpha\beta} \sim \mathcal{N} \frac{(\mathbf{q}_1 \mathbf{q}_2) q_3^2 + (\mathbf{q}_3 \mathbf{q}_1) q_2^2 + (\mathbf{q}_3 \mathbf{q}_2) q_1^2}{|q_1 q_2 q_3| q_p} \quad (6)$$

Taking into account the relation $\mathbf{q}_3 = \mathbf{k} - \mathbf{k}' - \mathbf{q}_1 - \mathbf{q}_2$, we can verify that $A_3^{\alpha\beta} \sim |\mathbf{k} - \mathbf{k}'|$. This is a common feature of all odd orders. In the case of single-phonon scattering, this causes the cross section to be proportional to $|\mathbf{k} - \mathbf{k}'|^2$.^[10] The cross sections of third and higher order have corrections proportional to $|\mathbf{k} - \mathbf{k}'|^2/q_0^2$, whereas the cross sections of even order have substantially smaller corrections, on the order of $\mathcal{N}^2 |\mathbf{k} - \mathbf{k}'|^2/q_0^2$. These corrections turn out to be small in the case of electron-hole pairs, since usually $|\mathbf{k} - \mathbf{k}'| \ll q_0^{\text{min}} \approx (2\mu l \Omega_{LO} / \hbar)^{1/2}$. However, as will be shown below, they become experimentally observable for odd-order cross sections in the frequency region below the absorption threshold, where the exciton states are significant.

The obtained asymptotic amplitudes (4) and (5) are the same both below the absorption threshold ω , $\omega' < \epsilon_g$, and above it, at ω , $\omega' > \epsilon_g$. However, the behavior of the cross sections of multiphonon processes turns out to be different in these two cases. In the region ω , $\omega' > \epsilon_g$ logarithmic singularities appear in the amplitude at the values $q_i \approx q_0$, due to the simultaneous vanishing of l denominators out of a total $(l+1)$. This l -fold resonance leads to a threshold-like increase of the cross section in the frequency interval from $\omega = \epsilon_g$ to $\omega' = \epsilon_g$, to the appearance of a dependence of the scattering cross sections on the damping of the electron system, and to a difference in the frequency dependences of the cross sec-

tions above and below the absorption threshold.

Figure 2 shows the results of numerical integration of the exact expression for $\sigma_2(\omega)$ at two values of the damping γ , which is introduced as a parameter by making the substitution $\Omega_p^{cv} \rightarrow \Omega_p^{cv} + i\gamma$. All the singularities noted above in the behavior of the cross section above the absorption threshold are clearly seen in the figure.

To estimate the magnitude of the jump at the threshold in the case of two-phonon scattering, we replace at ω , $\omega' > \epsilon_g$ the ratio of the differences of the logarithms to the differences of the arguments, which arises in (1) after integration with respect to p , by the derivative. This leads to the appearance, in the integral with respect to q , of the square of a smeared-out δ -function with an argument in the form $(q - q_0)$, so that the cross section above the threshold turns out to be of the order of

$$\sigma_2(\omega) \approx g \left(\frac{g \Omega_{LO}}{\gamma} \frac{q_0}{q_p} \right) \left(\frac{q_p}{q_0} \right)^6, \quad \omega, \omega' > \epsilon_g, \quad (7)$$

whereas below the threshold the estimates yield

$$\sigma_2(\omega) \approx g^2 (q_p/q_0)^7, \quad \omega, \omega' < \epsilon_g, \\ g = \frac{e^2}{2\hbar} \left(\frac{2\mu}{\hbar \Omega_{LO}} \right)^{1/2} \left(\frac{1}{\epsilon_\infty} - \frac{1}{\epsilon_0} \right). \quad (8)$$

Comparing the data of Fig. 2 with estimates based on formulas (7) and (8), we see that these approximate formulas provide a good estimate of the threshold jump $\sigma_2(\omega = \epsilon_g + 2\Omega_{LO})/\sigma_2(\omega = \epsilon_g)$ and describe qualitatively correctly the frequency dependence of the cross section.

Comparing (7) with the expression for the single-phonon cross section $\sigma_1(\omega)$, which is given by

$$\sigma_1(\omega) \sim g \frac{|\mathbf{k} - \mathbf{k}'|^2}{q_p^2} \left(\frac{q_p}{q_0} \right)^6, \quad (9)$$

we note that $\sigma_2(\omega)$ at ω , $\omega' > \epsilon_g$ can be of the order of the single-phonon cross section or may even be larger, if

$$\gamma \approx g \Omega_{LO} \text{ and } \frac{g \Omega_{LO}}{\gamma} \frac{q_0}{q_p} > \frac{|\mathbf{k} - \mathbf{k}'|^2}{q_p^2}.$$

If the relaxation of the electron excitations occurs mainly on LO phonons, then both conditions will be satisfied.

Both the threshold-like increase of the multiphonon processes and the dependence of the cross sections on γ at ω , $\omega' > \epsilon_g$ (and consequently on the temperature, on the defect concentration, etc.) can manifest themselves in experiment.

Allowance for the exciton structure

3. The Coulomb interaction of the electron and hole leads to the appearance of an exciton structure at the intrinsic absorption edge. Allowance for the Coulomb interaction in the scattering amplitude reduces to $(l+1)$ -fold summation of a ladder sequence. Carrying out this summation by the method of^[11], we obtain for the amplitude of l -phonon scattering by LO phonons the expression

$$A_l^{q\beta}(\omega) = \frac{(2\pi)^5 e^2 v_{\infty}^{\alpha} v_{\infty}^{\beta} (\Xi_{LO})' \psi_{\lambda_0}(0) \psi_{\lambda_l}(0)}{(\omega\omega')^{1/2} (\omega - E_{\lambda_0} - \varepsilon_g - \hbar k^2/2M)} \quad (10)$$

$$\times \delta(\mathbf{k} - \mathbf{k}' - \sum_{i=1}^l \mathbf{q}_i) \delta(\omega - \omega' - \sum_{i=1}^l \Omega_{q_i})$$

$$\times \prod_{m=1}^l (q_m d)^{-1} \frac{(e^{iq_m^c r} - e^{-iq_m^v r})_{\lambda_{m-1} \lambda_m}}{\omega_m - E_{\lambda_m} - \varepsilon_g - \hbar Q_m^2/2M}.$$

The symbol λ_m numbers here both the discrete states and the states of the continuous spectrum of the exciton.

$(l+1)$ -fold summation and integration with respect to $\lambda_0, \lambda_1, \dots, \lambda_l$, is implied in (10), in the form

$$\sum_{\lambda} (\dots) = \sum_{n=1}^{\infty} (\dots) + \int_0^{\infty} d(pa) (\dots), \quad (11)$$

where a is the Bohr radius of the exciton, E_{λ} is the energy of the relative motion of the electron and hole,

$$E_n = -R/n^2; \quad E_p = R(pa)^2; \quad R = \hbar^2/2\mu a^2.$$

The matrix element $(\dots)_{\lambda\lambda}$, in (10) is taken for the wave functions of the relative motion $\psi_{\lambda}(r)$.

The properties of the amplitudes (10) depend on which of the following four regions contains the frequencies ω and ω' :

$$\begin{aligned} \text{I } & \varepsilon_g - \omega; \quad \varepsilon_g - \omega' > 4\pi^2 R; \quad \text{I' } \omega - \varepsilon_g; \quad \omega' - \varepsilon_g > 4\pi^2 R; \\ \text{II } & \varepsilon_g - 4\pi^2 R < \omega, \omega'; \quad \omega \leq \varepsilon_g - R + \Omega_{LO}; \\ \text{III } & \varepsilon_g - R + \Omega_{LO} \leq \omega; \quad \omega, \omega' < \varepsilon_g + 4\pi^2 R. \end{aligned}$$

In regions I and I' the presence of an exciton structure is immaterial and the properties of the amplitude (10) are analogous to the case of free electrons and holes (1). Regions II and III are characterized by the fact that the main contribution to the amplitude is made here by exciton states that differ substantially from the states of free particles.

4. We consider now the cross section for single-phonon scattering in regions II and III. The amplitude (10) with $l=1$ contains one matrix element

$$\varphi_{\lambda\lambda'}(q) = \frac{1}{qa} (e^{iq^c r} - e^{-iq^v r})_{\lambda\lambda'}, \quad (12)$$

where $\mathbf{q} = \mathbf{k} - \mathbf{k}'$. Usually this expression is expanded in a series in $|\mathbf{k} - \mathbf{k}'|$ up to the first nonvanishing term, which is proportional to $|\mathbf{k} - \mathbf{k}'|a$.^[12, 13] It is seen from (12), however, that this leads to the appearance in the amplitude (10) of a diverging sum $\sum_n n^{-3} (r^2)_{\lambda\lambda}$ (since $r_{\lambda\lambda}^2 \sim n^4$) and of an analogous diverging contribution from the continuous spectrum of the exciton, so that we cannot use such an expansion. A more detailed examination shows that the contributions of the excitonic states to the amplitude increase with increasing principal quantum number n up to $n \approx n_0 = (\pi/2|\mathbf{k} - \mathbf{k}'|a)^{1/2}$. A similar increasing contribution is made by the continuous spectrum of the exciton when $1/pa$ increases to $1/pa \approx 1/p_0 a = n_0$. The contributions of states with $n > n_0$ and $1/p > 1/p_0$ oscillate rapidly and make a negligible contribution to the summation and integration in (10). Thus, the contribution to the amplitude of the exciton state depends

on the ratio of two characteristic dimensions—the wavelength of the phonon and the effective radius of the state and when the two coincide the contribution is resonantly intensified.

The matrix element $\langle e^{iq^c r} \rangle_{nn}$ is given by the expression

$$\langle e^{iq^c r} \rangle_{nn} = (-1)^{n-1} \frac{z^{2n-2}}{(1+z^2)^n} \frac{\sin(2n \arctg z)}{z} F\left(-n+1; -n+1; 2; -\frac{1}{z^2}\right), \quad (13)$$

where $z = nqa/2$ and F is a hypergeometric function.

Using the asymptotic form of F for large negative arguments, we can represent (13) in the form

$$\langle e^{iq^c r} \rangle_{nn} \approx \frac{1}{(z^2+1)^n} \frac{\sin(2n \arctg z)}{nz}, \quad (14)$$

so that the maximum contribution is made by the states whose number n is determined from the condition $2n \tan^{-1} z \approx \pi/2$, and the function begins to oscillate at values of n such that $2n \tan^{-1} z > \pi$.

For the continuous spectrum of the exciton at $q \ll p < 2\pi/a$, using the asymptotic form of a hypergeometric function with arguments close to unity, we obtain an analogous expression

$$\langle e^{iq^c r} \rangle_{pp} \approx \frac{pa}{(1-y^2)y} \sin\left(\frac{1}{pa} \ln \frac{1+y}{1-y}\right), \quad (15)$$

where $y = q/2p$. The maximum contribution is made by states with p determined from the condition

$$\frac{1}{pa} \ln \left(\frac{1+y}{1-y}\right) \approx \frac{\pi}{2},$$

and the oscillations begin at

$$\frac{1}{pa} \ln \left(\frac{1+y}{1-y}\right) > \pi.$$

Thus, the amplitude of the single-phonon scattering can be approximately represented in the form

$$A_l^{q\beta}(\omega) \approx \left\{ \sum_{n=1}^{n(\mathbf{k}-\mathbf{k}')} \frac{1}{\pi a^2 n^2} \frac{\varphi_{nn}(\mathbf{k}-\mathbf{k}')}{(\Delta(n) + i\gamma_n) (\Delta_1(n) + i\gamma_n)} + \frac{1}{\pi a} \int_{p(\mathbf{k}-\mathbf{k}')}^{\infty} \frac{p dp}{(1-e^{-2p/pa})} \frac{\varphi_{pp}(\mathbf{k}-\mathbf{k}')}{(\Delta(p) + i\gamma_p) (\Delta_1(p) + i\gamma_p)} \right\}, \quad (16)$$

where $\varphi_{nn}(q)$ and $\varphi_{pp}(q)$ are given by expressions (12), (14), and (15),

$$\Delta(\lambda) = (\omega - \varepsilon_g - E_{\lambda})/\Omega_{LO}; \quad \Delta_1(\lambda) = \Delta(\lambda) - 1;$$

γ_{λ} is the damping in units of Ω_{LO} . The values of $n(\mathbf{k} - \mathbf{k}')$ and $p(\mathbf{k} - \mathbf{k}')$ are determined from the condition

$$2n \arctg z \leq \pi \quad \text{and} \quad \frac{1}{pa} \ln \left(\frac{1+y}{1-y}\right) \leq \pi,$$

so that these limits turn out to be different for exponentials containing $|\mathbf{k} - \mathbf{k}'|^c$ and $|\mathbf{k} - \mathbf{k}'|^v$. The characteristic values n_0 at which the argument of the sine function in (14) is of the order of $\pi/2$ can be approximately estimated by expanding $\tan^{-1} z$. We then find that the size-dependent resonance takes place at $n \approx n_0 = (\pi/2|\mathbf{k} - \mathbf{k}'|a)^{1/2}$.

Since $|\mathbf{k} - \mathbf{k}'|$ is a relatively large quantity in the frequency region near the exciton (for CdS at $\omega \approx 2.5$ eV and $T = 4$ °K, in "backscattering" geometry, we have $|\mathbf{k} - \mathbf{k}'|/a \approx 0.24$), the corresponding values turn out to be not too large (at $|\mathbf{k} - \mathbf{k}'|/a = 0.24$ we have $n_0 \approx 2-3$).

As shown in [7,8], the size-dependent resonance manifests itself experimentally in a frequency dependence of the forbidden-scattering cross section, in a relative frequency dependence of the allowed and forbidden scattering, and in a dependence of the cross section of the forbidden scattering on the wave vector of the phonon $|\mathbf{k} - \mathbf{k}'|$, i.e., on the scattering geometry.

5. In the case of multiphonon processes, the scattering cross section can be represented in the form

$$\sigma_l(\omega) \approx \left[\frac{v_0}{(2\pi)^3} \right]^{l-1} \int \left(\prod_{m=1}^l d^3q_m \right) \delta \left(\mathbf{k} - \mathbf{k}' - \sum_{i=1}^l \mathbf{q}_i \right) \times \left\{ \sum P_{q_i} \right\} \left| \sum_{\lambda_0 \dots \lambda_l} \frac{\psi_{\lambda_0}(0) \psi_{\lambda_l}(0) \Phi_{\lambda_0 \dots \lambda_l}(q_1 \dots q_l)}{\Delta(\lambda_0) - \hbar k^2/2M\Omega_{LO} + i\gamma_{\lambda_0}} \right|^2 \delta \left(\omega - \omega' - \sum_{i=1}^l \Omega_{q_i} \right), \quad (17)$$

$$\Phi_{\lambda_0 \dots \lambda_l}(q_1 \dots q_l) = \prod_{m=1}^l \left[\frac{\Phi_{\lambda_{m-1} \lambda_m}(q_m)}{\Delta_m(\lambda_m) - \hbar Q_m^2/2M\Omega_{LO}} \right]. \quad (18)$$

The symbol $\left\{ \sum P_{q_i} \right\}$ stands for the $l!$ terms in (17) obtained as a result of summation of the topologically non-equivalent diagrams of the cross section in Fig. 1b. The term written out in (17) corresponds to diagram of Fig. 1b.

Expression (17) leads to different results in the frequency region above and below the absorption threshold, and qualitatively this difference has the same character as for free electrons and holes.

6. Region II is defined by us as the region above the absorption threshold, in which, however the exciton structure is already substantial. The lower limit of this region can be estimated from the following considerations. As follows from the expression (1) for the amplitude, in the case of free electron-hole pairs at $\omega < \varepsilon_g$, the main contribution to the integral with respect to p is made by the region

$$p \lesssim q_0 = (2\mu/\hbar)^{1/2} (|\varepsilon_g - \omega|^{1/2} + |\varepsilon_g - \omega'|^{1/2}).$$

Thus, even at a considerable distance from the threshold of the intrinsic absorption at $(\varepsilon_g - \omega)$, $(\varepsilon_g - \omega') \lesssim 4\pi^2 R$, the amplitude begins to receive its main contributions from the continuous-spectrum states with $p < 2\pi/a$ and from the discrete states of the exciton spectrum i.e., states that differ substantially from free electron-hole pairs.

As a result, the behavior of the amplitude as a function of the frequency and of the wave vectors of the phonons changes in comparison with the case of the free electrons and holes. The rate of increase of the amplitude as the frequency of the exciting light approaches the edge of the intrinsic absorption increases, and the region of the wave vectors of the phonons, which take part in the scattering, decreases. The phonon wave-vector values that are optimal in region II, can be estimated by starting from the properties of the form factors of the

exciton-phonon interaction. This estimate yields for the bound states of the exciton $q \lesssim 1/a$ and for the continuous spectrum $q \ll p < 2\pi/a$. If the relation between the binding energy of the exciton and the phonon frequency is such that the two inequalities $4\pi^2 R > \hbar\Omega_{LO} > R$, are simultaneously satisfied, then we can determine the region II for the cross section of scattering of order l , and phonons with wave vectors smaller than in the case of free electron-hole pairs will take part in the scattering in this region.

With increasing frequency, exact resonance appears first in one of the intermediate denominators in (17) and (18), and then in the rest of them. The lower limit of the region III was defined as the one above which $(l-1)$ intermediate denominators (17) can vanish at $\lambda_0 = \lambda_1 = \dots = \lambda_l = n = 1$:

$$\Delta_m(1) - \hbar Q_m^2/2M\Omega_{LO} = 0 \quad (m=1, 2, \dots).$$

Above this limit the terms of the discrete spectrum of the exciton in (17), containing the squares of moduli of such resonant denominators, become "gigantic," since the integrals of the type

$$\frac{v_0}{(2\pi)^3} \int d^3q \left[\left(\Delta_m(n) - \frac{\hbar q^2}{2M\Omega_{LO}} \right)^2 + \gamma_n^2 \right]^{-1} \sim \frac{(\Delta_m(n))^{1/2}}{\gamma_n} \quad (19)$$

diverge as $\gamma_n \rightarrow 0$. Thus, the region III is characterized by the fact that the intensity of the scattering depends on the damping of the electron system, and therefore to describe the scattering it becomes necessary to make some assumptions concerning the dependence of γ_λ on λ . For the subsequent calculations we assume that the minimum damping characterizes the ground state of the exciton $n=1$. Then, using the property of the integrals (19), we can pick out of the general expression (17) the terms that are maximal with respect to the parameter $\Delta_m(n)/\gamma_n$ and yield the "imbedded" diagrams of Fig. 1b at $\lambda_0, \lambda_1, \dots, \lambda_l = n = 1$:

$$\sigma_l(\omega) \sim \left[\frac{v_0}{(2\pi)^3} \right]^{l-1} \int \left(\prod_{i=1}^l d^3q_i \right) \delta \left(\mathbf{k} - \mathbf{k}' - \sum_{i=1}^l \mathbf{q}_i \right) \delta \left(\omega - \omega' - \sum_{i=1}^l \Omega_{q_i} \right) \times \left| \frac{1}{\Delta - \hbar k^2/2M\Omega_{LO} + i\gamma} \prod_{m=1}^l \frac{\Phi(q_m)}{\Delta_m - \hbar Q_m^2/2M\Omega_{LO} + i\gamma} \right|^2, \quad (20)$$

$$\Delta = \Delta(1); \quad \Delta_m = \Delta_m(1); \quad \Delta_m(\lambda) = \Delta(\lambda) - m; \quad \gamma = \gamma_1; \quad \Phi(q) = \Phi_{11}(q).$$

We note that it follows from (20) and (19) that the wave vectors of the phonons that take part in the scattering in region III turn out, unlike in region II, to be dependent on the frequency

$$q = (2M\Omega_{LO}\Delta_m/\hbar)^{1/2}.$$

We consider now the frequency dependences of the cross sections of multiphonon processes in regions II and III, as well as their dependences on l .

7. In region III we confine ourselves to the approximate expression (20). Using (19), we transform (20) into

$$\sigma_l \sim \frac{g^2 \mathcal{M}^2}{(\Delta^2 + \gamma^2)(\Delta^2 + \gamma^2)} \frac{\Gamma(\Delta_1 \dots \Delta_{l-1})}{\gamma(\Delta_1)\gamma(\Delta_2) \dots \gamma(\Delta_{l-1})}, \quad (21)$$

$$\Gamma = \left[\frac{g^2 \mathcal{M}^2 a^3}{4\pi} \right]^{l-1} \int \left[\prod_{i=1}^{l-1} d^3 q_i \delta \left(\Delta_i - \frac{\hbar q_i^2}{2M\Omega_{LO}} \right) \right] \times \varphi^2(q_1) \varphi^2(q_1 - q_2) \dots \varphi^2(q_{l-2} - q_{l-1}) \varphi^2(q_{l-1}). \quad (22)$$

Carrying out the integration in (22) we obtain

$$\Gamma = g^2 \mathcal{M}^2 \Delta_i^{1/2} \varphi^2(\Delta_i) \varphi^2(\Delta_{l-1}) \gamma^0(\Delta_i) \dots \gamma^0(\Delta_{l-2}), \quad (23)$$

$$\gamma^0(\Delta_i) = \frac{g^2 \mathcal{M}^2}{4\Delta_i^{1/2}} \int_{y_i^-}^{y_i^+} dy \varphi^2(y), \quad \varphi^2(y) = \frac{M}{\mu} by \frac{[1 + 1/2(\alpha + 1/\alpha)by]^2}{[1 + \alpha by]^4 [1 + by/\alpha]^4}, \quad (24)$$

$$y_i^\pm = (\Delta_i \pm \Delta_{i+1})^2; \quad \alpha = m_c/m_v; \quad b = \Omega_{LO}/4R; \quad g^2 = g/(q_p a);$$

$\gamma^0(\Delta_i)$ stands for the probability of emission of an LO phonon for an exciton situated in the ground state $n=1$ with kinetic energy $(\Delta_i \Omega_{LO})$.

Using (23), we write down (21) in the form

$$\sigma_l(\omega) \sim \frac{g^2 \mathcal{M}^2 \varphi^2(\Delta_{l-1})}{(\Delta^2 + \gamma^2)(\Delta_i^2 + \gamma^2)} \left[\frac{g^2 \mathcal{M}^2 \Delta_i^{1/2} \varphi^2(\Delta_i)}{\gamma(\Delta_{l-1})} \right] \prod_{i=1}^{l-2} \frac{\gamma^0(\Delta_i)}{\gamma(\Delta_i)}. \quad (25)$$

If the main exciton-relaxation channel is emission of LO phonons, then the expression under the product sign does not decrease very rapidly with increasing l .

Figure 3 shows the result of the calculation of the frequency dependence of the cross sections of orders 2–5 in accordance with formula (25). In the calculation, the ratios $\gamma^0(\Delta_i)/\gamma(\Delta_i)$ were set equal to unity. As seen from the figure, the theory predicts in this case a weak dependence of the cross sections on l in a wide frequency interval, in qualitative agreement with the experimental results.^[1,2] We note that just as in the case of free electrons and holes in the region $\omega, \omega' > \varepsilon_g$, the cross section of order l is effectively transformed in region III into a first-order process, inasmuch as the expression in the square brackets of (25) depends little on the coupling constant g^e (since $\gamma \sim g^e$ in this case, too).

8. We consider now the behavior of multiphonon processes in region II. As shown in the calculation of the amplitude of the single-phonon scattering, the diagonal matrix elements $\varphi_{\lambda\lambda}(q)$ increase with increasing n and with decreasing p , and this growth continues up to $n \approx (qa)^{-1/2}$ and $pa \approx (qa)^{1/2}$, where q is the wave vector of the phonon. For subsequent estimates we shall use the asymptotic form of $\varphi_{\lambda\lambda}(q)$ as $q \rightarrow 0$, which is given for discrete states by

$$\varphi_{nL, n'L'}(q) \sim \begin{cases} 3/3 \mathcal{M}(aq) n^4 \delta_{nn'} & \text{if } L=L' \\ 3/2 n^2 \delta_{nn'} & \text{if } L=L' \pm 1 \end{cases} \quad (26)$$

(L and L' are the orbital quantum numbers), and an analogous expression for the continuous spectrum.

In contrast to the single-phonon process, in the multiphonon process the value of the wave vector of the phonon can be arbitrarily small. The square of the modulus of the amplitude, which contains sums in the form $|\sum_{n=1}^{n_{\max}} [\varphi_{nn}(q)]^2|$, tends to unity like $(qa)^{-2l+2}$ as $q \rightarrow 0$, and the integral over the continuous spectrum behaves in similar fashion. This divergence is eliminated by decreasing the volume of the phase space of the wave vectors of the phonon in the $(l-1)$ -fold integration with respect to q_i . Thus, in the estimates we can assume an upper summation limit $n_{\max} \approx (aq)^{-1/2}$, a lower integra-

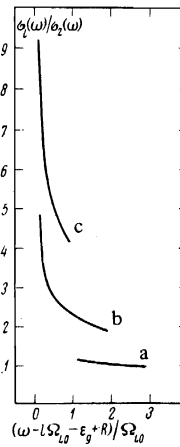


FIG. 3. Frequency dependence of the cross section ratios $\sigma_l(\omega)/\sigma_2(\omega)$ in region III for $l=3, 4, 5$ (a, b, c). The scattering cross sections are corrected for the absorption of the incident and scattered light for "backward" geometry; the absorption coefficient is assumed proportional to $\gamma_0/[(\omega - \varepsilon_g + R)^2 + \gamma_0^2]$, and γ_0 is taken equal to $0.1 \Omega_{LO}$.

tion $(pa)_{\min} \approx (qa)^{1/2}$, and the upper integration limit can be replaced by infinity. We can integrate with respect to the wave vectors of the phonons from zero to $q_{\max} \sim 1/a$.

From (26) follow differences in the behavior of the cross sections of even and odd order, similar to those in the excitonless case.²⁾ For even-order cross sections we can set up chains of intermediate states of alternating parity $s-p-s, s-p-s-p-s$ etc. At the same time, for odd-order processes it is necessary to include in the chain at least one matrix element $\varphi_{nL, nL}(q)$ between states of like parity: $s-p-s-s, s-s-p-s, s-p-p-s$ etc. (in the general case there are l different possibilities), inasmuch as the first and last state should be of the s type.

Inclusion, of a matrix element between states of like parity in the chain of states leads, first, to the appearance of a factor $\mathcal{M}^2 \ll 1$ in the odd-order cross sections and, second, to their dependence on the wave vector transferred to the phonon system. A term proportional to $|\mathbf{k} - \mathbf{k}'|^2$ appears in the odd-order cross sections, as a result of the proportionality of the matrix element $\varphi_{nL, nL}(q)$ to the wave vector of the phonon, after substitution of the expression for one of the q_i in terms of $(\mathbf{k} - \mathbf{k}')$ in the remaining $(l-1)$ vectors q_i and after integration of q_i over the angles. Inasmuch as a similar term appears in even-order cross sections when two matrix elements are placed between states of like parity, its relative contribution will be much less.

The scattering cross sections at $\varepsilon_g - R - \omega \gtrsim R, \varepsilon_g - \omega, \varepsilon_g - \omega' < 4\pi^2 R$ can be approximately represented in the form

$$\sigma_l \approx \left(\frac{3}{2} \right)^{2l} \frac{(g^e)^{2l} l!}{(l-1)^2 (l-1)! \Delta^2 \Delta_i^2 \dots \Delta_i^2} \frac{1}{\Delta^2 \Delta_i^2 \dots \Delta_i^2} \quad \text{if } l \text{ is even}, \quad (27a)$$

$$\sigma_l \approx \left(\frac{5}{3} \mathcal{M} \right)^2 \left(\frac{3}{2} \right)^{2(l-1)} \frac{(g^e)^{2l} l! l^2}{l^2 (l-1)! \Delta^2 \Delta_i^2 \dots \Delta_i^2} \frac{[1 + c|\mathbf{k} - \mathbf{k}'|^2 a^2]}{\Delta^2 \Delta_i^2 \dots \Delta_i^2} \quad \text{if } l \text{ is odd}, \quad (27b)$$

where c is a quantity of the order of unity.

A limit has been imposed on the frequency ω because in the derivation of (27) we have neglected quantities of order R in all the intermediate denominators. The factor $l!$ in the numerators of (27) takes into account the number of topologically non-equivalent diagrams in the cross section (Fig. 1b). The factors $(l-1)^2$ and l^2 in

the denominators of (27) are due to estimates of sums of the form

$$\sum_{n=1}^{n_{\max}} n^{2l-3} \approx \frac{n_{\max}^{2l-2}}{(2l-2)}; \quad \sum_{n=1}^{n_{\max}} n^{2l-1} \approx \frac{1}{2l} n_{\max}^{2l}$$

in the even and odd orders, respectively. The factors $(l-1)!$ in the denominators of (27) are the result of an estimate of multiple integrals of the type

$$\int_0^1 d(q_1 a) d(q_2 a) \dots d(q_{l-1} a) \approx \frac{1}{(l-1)!}.$$

Such an estimate of the integrals leads to minimal values of σ_l . The factor l^2 in the numerators of the odd-order sections reflect l different possibilities of including $\varphi_{nL, nL}(q)$ in the amplitude.

From a comparison of (27a) and (27b) it is seen that the factor \mathcal{M}^2 can lead to an irregular decrease of the cross section of order l . If $\mathcal{M}^2(l-1)^2 < 1$, then the cross section of odd order l will be closer in magnitude to σ_{l+1} than to σ_{l-1} . If this condition is not satisfied, however, then this indicates that besides the chains of intermediate states with minimal number of matrix elements between the states of like parity it is necessary to take into account also chains that contain a larger number of such matrix elements. The dependence of σ_l on l then turns out to be smoother.

When the excitation frequency approaches the level $n=1$ of the exciton, we can retain in the expressions for the amplitudes only those chains which begin with the state $1s$. This ensures matching of the results in regions II and III. In the limit as $\omega \rightarrow \varepsilon_g - R$ the expressions for the amplitudes become simpler and the estimates of the cross sections and of their dependence on l can be obtained in a different manner. Obviously, in this case the scattering amplitude will be close in its properties to the amplitude of the luminescence for the state $n=1$; we consider here only the behavior of multiphonon luminescence bands.

9. Calculation of the cross section of the luminescence processes is perfectly analogous to the preceding analysis, with the exception of the fact that the changes of the intermediate states begin and end with the state $1s: 1s-1s$ for σ_1 ; $1s-2p-1s$ and $1s-1s-1s$ for σ_2 ; $1s-2p-1s-1s$, $1s-2p-2p-1s$, $1s-1s-2p-1s$ for σ_3 and $1s-2p-1s-2p-1s$ for σ_4 . The approximate formulas for the cross sections can be represented in the form

$$\begin{aligned} \sigma_1 &\approx g^2 \mathcal{M}^2(k_1 a)^2; \quad \sigma_l \approx (g^2)^l \frac{I_l}{l!} \quad \text{for even } l \\ \sigma_l &\approx (g^2)^l \mathcal{M}^2 [1 + c' (k_1 a)^2] \frac{I_l}{l!} \quad \text{for odd } l, \end{aligned} \quad (28)$$

where \mathbf{k}_T is the wave vector of the excitons, T is the exciton temperature, I_l is an integral, with respect to the wave functions of the phonons, of the product of the form factors of the exciton-phonon interaction, for the above-listed chains of the intermediate states, and c' is a constant of the order of unity.

In the derivation of (28) we have taken the amplitude denominators outside the integral with respect to the

wave vectors of the phonons, and have neglected quantities of order R in these denominators; this is valid if $\Omega_{LO} > R$. After averaging over the thermal distribution of the excitons, we obtain

$$\begin{aligned} \sigma_l &\approx \frac{3}{2} \xi T g^2 \mathcal{M}^2; \quad \sigma_l \approx (g^2)^l \frac{I_l}{l!} \quad \text{for even } l. \\ \sigma_l &\approx \left(1 + \frac{3}{2} c' \xi T\right) (g^2)^l \frac{I_l}{l!} \quad \text{for odd } l, \end{aligned} \quad (29)$$

where $\xi = 2M\alpha^2/\hbar^2 = M/\mu\hbar R$.

In the estimate of σ_l we can break up the multiple integrals into products of single integrals, which can be calculated exactly. This procedure overestimates the values of σ_l . The estimated intensity distributions for multiphonon scattering lines, in accordance with formulas (27) and for the luminescence band from the state $n=1$ of the exciton in accordance with formula (29), will be presented below together with the experimental data. There is good agreement between these different estimates.

10. We note an interesting property of the multiphonon luminescence cross sections, which can be obtained in the limit $\Omega_{LO} \ll R$ at $m_v \gg m_c$. In this case we can retain as the intermediate state only $n=1$, and then σ_l can be represented in the form

$$\sigma_l \approx (g^2)^l S^l / l!, \quad (30)$$

where $S^l = I_l$, which agrees with Pekar's formula^[14] for the intensity distribution of electron-vibrational spectra of impurity centers. Indeed, in this limiting case the exciton is self-localized and is similar to an impurity center with one excited level.

We note in conclusion that the dependence of the multiphonon-scattering cross section on the momentum transferred to the phonon system $|\mathbf{k}-\mathbf{k}'|$, at frequencies below their absorption threshold, and the corresponding dependence of the multiphonon thermalized-luminescence cross sections, follow from the following property of the matrix elements of the exciton-phonon interaction: the matrix element between states of large parity (between states of s type, since we are considering dipole-allowed scattering and luminescence) of a product of an odd number of $\varphi(q)$ is proportional to

$$\langle s | \varphi(q_1) \varphi(q_2) \dots \varphi(q_l) | s \rangle \sim [|\mathbf{k}-\mathbf{k}'| a]^l \mathcal{M}, \quad (31)$$

whereas the matrix element of a product of an even number of $\varphi(q)$ does not depend on $|\mathbf{k}-\mathbf{k}'|$. This property holds for all values of q_i which are connected with the wave-vector conservation law. However, only in the region below resonance and at $q_i a \ll 1$ (at $q_i \ll q_0$ in the case of free electrons and holes) is the behavior of the amplitude close to the behavior of the matrix element of the products of the form factors $\varphi(q_i)$. In this limiting case the dependence of the intermediate denominators of the amplitude on the quantum number λ_i becomes insignificant, since the main contribution is made by large n and small p .

III. EXPERIMENTAL RESULTS AND DISCUSSION

Experimental procedure

We have investigated the purest and most perfect CdS and CdSe at our disposal, grown from the gas phase. The line widths of the forbidden excitonic transitions and of the additional spikes in the excitonic reflection spectra^[15] of these crystals did not exceed 10^{-4} eV, thus attesting to the high degree of their perfection. The spectra of the investigated samples did not contain at all donor-acceptor pair radiation, and this enables us to observe the relatively weak multiphonon-scattering and multiphonon exciton luminescence spectra in a wide spectral range.

The exciton-phonon luminescence spectra of the crystals CdS and CdSe was excited with light from the region of the intrinsic absorption. It turned out that the shapes of these spectra and the relative intensity of the different lines did not depend on the spectral composition, on the polarization, or on the intensity of the exciting light. The Raman-scattering spectra of the CdS crystals were investigated in polarized light using the line $\lambda_L = 4880 \text{ \AA}$ of an Ar⁺ laser in a "backward" or "forward" scattering geometry. In this case, in agreement with Martin's results,^[12] the intensity of the scattering in a polarization parallel to the polarization of the exciting light (forbidden scattering) is approximately 10 times larger than in crossed polarizations. We shall henceforth discuss only the data obtained in parallel polarizations. The scattering geometry is characterized in this case by the orientation of the polarization of the light relative to the hexagonal axis of the crystal *C* (the *z* direction), which lies in the plane of the investigated samples. In the case of **E** || *C* polarization (*xzzx* geometry), optical transitions are allowed into the excitonic states of the series *B* ($\Gamma_7-\Gamma_7$) and *C* ($\Gamma_7-\Gamma_7$), and the shift of the exciting frequency relative to the nearest excitonic state $n=1B$ ($\lambda = 4825 \text{ \AA}$) amounts to 240 cm^{-1} at helium temperatures. In **E** ⊥ *C* polarization (*x(yy)x* geometry), transitions into the excitonic states of the series *A* ($\Gamma_9-\Gamma_7$) are also active. The shift of the exciting frequency relative to the state $n=1A$ ($\lambda = 4857 \text{ \AA}$) is in this case only $\sim 100 \text{ cm}^{-1}$. Scattering in **E** ⊥ *C* polarization has a more resonant character, and the intensity of all the Raman-scattering lines in this case approximately 10 times larger than in the polarization **E** || *C*.

Raman scattering of first order by LO phonons

In Raman scattering of perfect CdS samples there is observed a narrow 1LO line of width $\sim 1 \text{ cm}^{-1}$. Depending on the crystal orientation, it is possible to observe excitation of phonons of symmetry A_1 or E_1 at 302.6 and 305.7 cm^{-1} , respectively. The intensity of the 1LO "forward" scattering line is approximately half that of the "backward" line, this being due to the dependence of the cross section of the 1LO scattering on the value of the wave vector transferred to the phonon system of the crystal.^[16] Owing to the appearance of the size-dependent resonance, the ratio of the contribution that depends on $|\mathbf{k}-\mathbf{k}'|$ to the first-order scattering cross section to the independent contribution depends on the proximity of

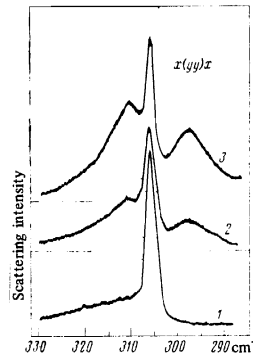


FIG. 4. Spectrum of Raman scattering of light ($\lambda_L = 4880 \text{ \AA}$) by a CdS crystal in the region of first order with respect to the LO phonon in a geometry *x*(*yy*)*x* at different temperatures: 1—2; 2—20; 3—40 K.

the frequency of the exciting light to the frequencies of the excitonic transitions.^[18] When the excitation frequency moves away from the state $n=1$ of the exciton, a rapid redistribution of the relative contributions of the parts dependent on and independent of $|\mathbf{k}-\mathbf{k}'|$ to the cross section takes place in such a way that even at $\epsilon_g - R - \omega \approx 2\Omega_{LO}$ the cross-section component independent of $|\mathbf{k}-\mathbf{k}'|$ amounts to approximately 90% of the total scattering cross section. On moving farther into the regions I and I', the proportionality of the cross section of single-phonon scattering to the quantity $|\mathbf{k}-\mathbf{k}'|^2$ is restored.

One more interesting feature of scattering in the single-phonon region is illustrated in Fig. 4, which shows the 1LO line in the "forward" scattering geometry *x*(*yy*)*x* (phonon symmetry E_1) at various temperatures. At $T = 2 \text{ K}$ a wing is observed on the long-wave side of the line; it is due, in our opinion, to the simultaneous excitation of optical and acoustic phonons in the scattering act. With increasing temperature, the intensity of this wing increases, and on the short-wave side there appears an anti-Stokes Raman-scattering band due to the absorption of acoustic phonons from the crystal lattice. The shift of the maximum of this band relative to the 1LO line is approximately 8 cm^{-1} and makes it possible to estimate the wave vectors of the phonons having the maximum two-phonon scattering probability. Assuming that the interaction is with LA phonons,^[17] these vectors have values on the order of 5×10^{-2} of the limiting value of the vector at the boundary of the Brillouin zone. This value is close to the reciprocal Bohr radius of the free excitons $n=1A$, which agrees well with the assumptions advanced earlier.^[18]

Multiphonon Raman scattering with excitation of LO phonons

The absence of donor-acceptor pairs from the spectra of the investigated luminescence centers has enabled us to investigate the spectrum of multiphonon Raman scattering of CdS crystals in a wide spectral region. Under the conditions of resonant excitation, the Raman-scattering spectrum reveals, besides the 1LO line, also the relatively narrow lines 2LO, 3LO, and 4LO, which are displaced from the exciting line by an energy that is a multiple of the LO-phonon energy at the center of the Brillouin zone (Fig. 5).

Table I lists the values of the shift, the half-width,

TABLE I. Characteristics of lines of multiphonon scattering of light in CdS crystal.

Order of scattering	1	2	3	4	
Energy shift, cm^{-1}	305.7	611	917	1219	
Half-width, cm^{-1}	2.1	7.8	8.3	9	
Relative intensity	experiment	0.064	1	0.013	0.0016
	theory	0.16	1	0.018	0.0013

Note. Scattering geometry $x(yy)\bar{x}$, $\lambda_L = 4880 \text{ \AA}$, $T = 2 \text{ K}$. Data on the half-width are given without correction for the apparatus function, the experimental resolution is $\sim 1 \text{ cm}^{-1}$. The theoretical estimates are based on formulas (27) using the following values of the parameters: $g^e = 0.5$; $M^2 = 0.1$.

and the relative intensity of the LO lines of multiphonon scattering when CdS crystals are excited by the 4880 \AA line at $T = 2 \text{ K}$. As seen from this table, the probability of the multiphonon Raman-scattering processes decreases rapidly with increasing number of the order. The observed distribution of the relative intensity differs substantially from the distribution of the intensity of the multiphonon lines upon excitation in the regions of the intrinsic absorption. In this case^[1, 2, 19] lines are also observed shifted by an energy 2, 3, 4, etc. LO phonons relative to the exciting line, but lines with close numbers have comparable intensities. In the case of excitation below resonance, the most intense line in the spectrum of the multiphonon scattering is the 2LO line (the intensity of this line was used in Table I to normalize the intensities of all the remaining lines). The strength of the 3LO line is approximately one-hundredth that of the 2LO lines. At the same time, the 4LO line is weaker than the 3LO line by only a factor of 10. Such an irregular character of the variation of the intensity, as noted in item 8 of the preceding section, is due to the appearance in the scattering cross sections of odd orders of the factor M^2 , which is equal to 0.1 for CdS.

An estimate of the intensity of the multiphonon LO-scattering lines by formulas (27) describes qualitatively correctly the observed distribution of the intensity (see Table I).

It should be noted that the relative intensity of the lines 1LO and 3LO (relative to 2LO) depends on the degree of perfection of the sample^[16] and increases when defects are introduced. The introduction of defects does violence to the law of wave-vector conservation in scattering processes, thereby increasing effectively the wave

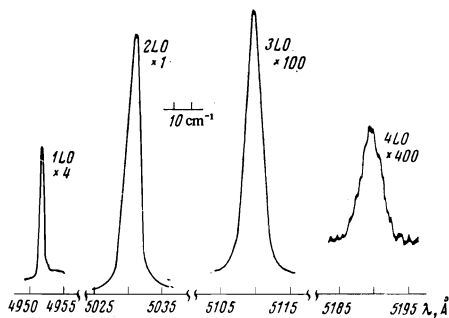


FIG. 5. Spectrum of multiphonon scattering of light ($\lambda_L = 4880 \text{ \AA}$) by a CdS crystal. Scattering geometry $x(yy)\bar{x}$, $T = 2 \text{ K}$.

vector transferred to the phonon system. In addition, the additional act of scattering of an exciton by an impurity can convert a scattering process of order l into a process of order $(l+1)$.^[20] Both factors lead to a substantial increase of the intensities of the odd orders of scattering below the intrinsic-absorption edge (and of the first order in the region above the edge^[21]). Indeed, the odd-order scattering cross section (see formula (27b)) depends on the value of $|\mathbf{k} - \mathbf{k}'|$ and contains a small factor M^2 , which is missing in even-order cross sections. An even-order scattering cross section should not be very sensitive to the action of the indicated factors. This circumstance has enabled us to use the intensity of the 2LO line to normalize the intensities of the remaining lines. The dependence of the odd-order scattering cross section on $|\mathbf{k} - \mathbf{k}'|$ is most clearly pronounced in the investigation of the exciton-phonon luminescence.

Multiphonon luminescence of free excitons

In the case of excitation above the intrinsic absorption edge, we observed in all the investigated CdS and CdSe crystals an intense luminescence of the free excitons, and the spectrum of this luminescence did not depend on the frequency of the exciting light, thus attesting to its quasi-equilibrium character. We observed in the spectrum both phononless luminescence lines (these lines are not considered in the present paper) as well as lines of annihilation of excitons $n = 1A$ with simultaneous excitation of one or several LO phonons ($A_1 - lLO$). In addition to the lines $A_1 - LO$ and $A_1 - 2LO$, which were investigated in detail earlier,^[18, 22] we succeeded in observing much weaker lines $A_1 - 3LO$ and $A_1 - 4LO$. This distribution of the relative intensity of the lines $A_1 - lLO$ has a similar character in the crystals CdS and CdSe (Table II).

With increasing crystal temperature, characteristic changes take place in the exciton-phonon luminescence spectra. First, all the $A_1 - lLO$ lines broaden and acquire a characteristic Maxwellian shape (Fig. 6). Second, a change takes place in the distribution of the relative intensities of the different lines, mainly, of the integral intensities of the lines $A_1 - LO$ and $A_1 - 3LO$ in comparison with the lines $A_1 - 2LO$ and $A_1 - 4LO$.

The ratio of the integral intensities of the lines $A_1 - 2LO$ and $A_1 - 4LO$ does not depend on the temperature (Fig. 7). An analysis of the line contours at different temperatures shows that the shape of the line $A_1 - 4LO$,

TABLE II. Relative intensity exciton-phonon luminescence lines of the crystals CdS and CdSe.

	T, K	1LO	2LO	3LO	4LO
CdSe	1.6	1.2	1	0.016	0.0016
CdS	1.6	0.7	1	0.015	0.0017
CdS	30	3	1	0.03	0.002
CdS, theor.	30	3	1	0.04	0.008

Note. The theoretical estimates were performed for a CdS crystal in accordance with formulas (29), using the following values of the parameters: $M = 1.55$; $\mu = 0.18$, $R = 28 \text{ meV}$; $c' = 1$; $g^e = 0.5$.

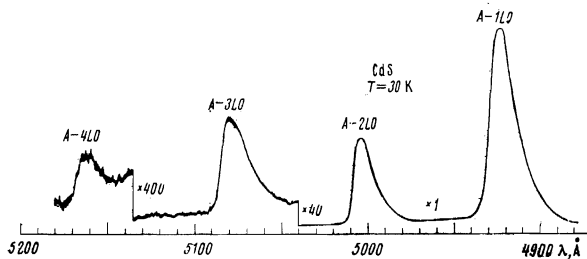


FIG. 6. Spectrum of exciton-phonon luminescence of CdS crystal at $T=30$ K.

just as the shape of the line A_1-2LO , is well described by the Maxwell formula $E^{1/2} \exp(-E/k_B T)$, where E is the kinetic energy of the exciton. It can thus be concluded that an equilibrium distribution of the excitons with respect to the kinetic energy is established in the investigated CdS and CdSe samples. At the same time the Maxwellian shape of the lines A_1-2LO and A_1-4LO indicates that the probability of two- and four-phonon annihilation of the excitons does not depend on the wave vector of the exciton. This result agrees with the already noted fact that the even-order Raman-scattering cross section is independent of the quantity $|\mathbf{k}-\mathbf{k}'|$. Figure 8 shows the temperature dependence of the half-width of the lines A_1-1LO . As seen from the figures, the widths of the lines A_1-2LO and A_1-4LO increase linearly with increasing temperature, and the slope of this increase amounts to $1.8 k_B$ (k_B is the Boltzmann constant); this agrees with the result expected for a Maxwellian contour (dash-dot line 1 of Fig. 8). In addition, the lines A_1-2LO and A_1-4LO have a certain additional broadening that does not depend on the temperature. This broadening is apparently due to the existence of a "bottleneck" region^[23] near the bottom of the band $n=1A$, for which no thermal equilibrium was established.^[24] This additional broadening is approximately twice as large in CdS than in CdSe (see Fig. 8), a fact reflecting the relative values of the longitudinal-transverse splitting in these crystals, 16 and 7.7 cm^{-1} , respectively.^[15,25]

The contour of the A_1-LO line is well described by the formula $E^{3/2} \exp(-E/k_B T)$, and the half-width of this line, in both CdS and CdSe, varies in accordance with this dependence (dashed line 2 on Fig. 8 with slope $3.1 k_B$), while the relative intensity (normalized to the intensity of the line A_1-2LO) increases linearly with tem-

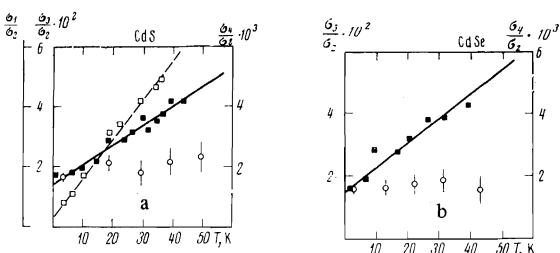


FIG. 7. Temperature dependence of the ratio of the integrated intensities of first (\square), third (\blacksquare), and fourth (\circ) order to the intensity of the second-order band of the exciton-phonon luminescence of the crystals CdS (a) and CdSe (b).

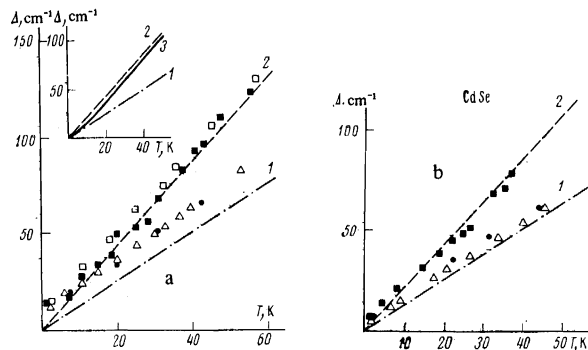


FIG. 8. Temperature dependence of the half-width of the exciton-phonon luminescence bands of various orders of the crystals a—CdS and b—CdSe, \square — A_1-1LO ; Δ — A_1-2LO ; \blacksquare — A_1-3LO ; \bullet — A_1-4LO . Lines 1 and 2—temperature dependences of the half-widths of the contours of $E^{1/2} \exp(-E/k_B T)$ and $E^{3/2} \exp(-E/k_B T)$ respectively. Curve 3 (insert)—temperature dependence of the contour of $(1+\xi E)E^{1/2} \exp(-E/k_B T)$ at $\xi=0.034 \text{ deg}^{-1}$.

perature.^[22] The appearance of an additional factor E in the formula describing the shape of the line A_1-LO , reflects the dependence of the probability of the single-phonon scattering on the value of the wave vector transferred to the phonon. In the region of sufficiently large values of the wave vectors $|\mathbf{k}-\mathbf{k}'|$ characterizing thermal excitons, when account is taken of the parabolic dispersion of the exciton band, this dependence can be represented in the form^[18]

$$\sigma_1 \sim |\mathbf{k}_T - \mathbf{k}'|^2 \sim k_T^2 \sim E. \quad (32)$$

The line A_1-3LO has a more complicated temperature dependence. Its relative intensity also changes with temperature in linear fashion, but much more slowly than for the A_1-LO line. The half-width of the line A_1-3LO varies with temperature practically in the same way as for the line A_1-LO . Taking into account the presence of a contribution proportional to k_T^2 in the third-order exciton-phonon scattering cross section, the spectral shape of the A_1-3LO line can be represented by the formula

$$\Phi_3(E) \sim (1+\xi E)E^{3/2} \exp(-E/k_B T). \quad (33)$$

The coefficient ξ , which describes the relative magnitude of the contribution proportional to k_T^2 to the scattering cross section, can be determined from the temperature dependence of the relative intensity of the line A_1-3LO . It is easy to show that the dependence expected in the case of the contour (33) is described by the expression $\sigma_3/\sigma_2 \sim (1+\frac{3}{2}\xi T)$. The coefficient ξ determined from the analysis of the experimental data shown in Fig. 8 is equal to 0.034 and 0.041 deg^{-1} in the crystals CdS and CdSe, respectively. An estimate of ξ , based on formula (29), yields values 0.026 and 0.037 respectively for CdS and CdSe. The temperature dependence of the half-width of the contour (33), calculated with the same values of the coefficient ξ , practically coincides with the temperature dependence of the half-width of the $E^{3/2} \exp(-E/k_B T)$ contour (curves 3 in the insert of Fig. 8).

IV. CONCLUSION

The investigation of the multiphonon resonant LO scattering in CdS crystals and its comparison with exciton-phonon luminescence of CdS and CdSe crystals show that the main regularities of the observed scattering are determined in this case by resonance with free excitons that are intermediate states in the Raman-scattering process. By virtue of the universal character of the hydrogen-like spectrum of the intermediate states and of the Frohlich interaction of the excitons with the LO phonons, analogous regularities should be observed also in the spectra of resonant Raman scattering of other crystals having a sufficiently high degree of ionicity and sufficiently high binding energy of the free excitons. Multiphonon exciton-luminescence and resonant Raman-scattering spectra in region II have a similar distribution of the relative intensity (see Tables I and II). In addition, for both types of spectra there are observed identical differences in the dependence of the cross sections of even and odd orders on the wave vector.

It is interesting to note that the cross section of resonant Raman scattering of any order contains generally speaking, both a part that does not depend on the value of the wave vector $|\mathbf{k} - \mathbf{k}'|$, and a part proportional to the square of the vector $|\mathbf{k} - \mathbf{k}'|^2$. In even scattering orders, as shown by investigations of the Raman-scattering and exciton-phonon-luminescence spectra, the dependence of the scattering cross section on $|\mathbf{k} - \mathbf{k}'|^2$ is very weak and can be disregarded in practice. The strongest dependence on $|\mathbf{k} - \mathbf{k}'|^2$ is possessed by the first order in the region of the polariton resonance.^[15] The constant (independent of $\mathbf{k} - \mathbf{k}'$) part of the cross section amounts here, in accordance with the estimate made in^[6], to about 2% of the total value of the cross section (the damping of the excitonic state $n = 1A$ is equal to $\gamma_{1s} = 0.02\Omega_{LO}$) and consequently at low temperatures it can be disregarded in practice in this frequency region.

In third-order scattering, the dependence of the cross section on the wave vector is weak at any distance from resonance. However, when the value of $|\mathbf{k} - \mathbf{k}'|$ is substantially increased (for example, in the spectra of the exciton-phonon luminescence at high temperatures), this dependence becomes quite discernable.

Our theoretical analysis shows that the different dependences of the even- and odd-order LO scattering cross sections on the wave vector are due to the difference in the character of the alternation of the intermediate states of the s and p type. Since odd orders must include one scattering process between states of like parity, the cross section of such a process contains a contribution that depends on $|\mathbf{k} - \mathbf{k}'|$, as well as a factor \mathcal{N}^2 , which leads, in the case when the effective masses of the electron and hole are close in magnitude, to an irregular distribution of the intensities of the multiphonon lines. In the limiting case when the carriers making up the exciton have equal effective masses, the intensity of odd-order light scattering by LO phonons should be equal to zero.

It should be noted in conclusion that an investigation of the resonant Raman scattering provides much in-

formation on exciton-phonon interaction processes. The main features of the observed phenomena are determined by the universal properties of the excitonic and phonon spectra and should be common to a large class of crystals.

¹⁾Successive emission of phonons leads to a stronger dependence of the cross section on the frequency, i. e., to a more resonant behavior of the cross section.

²⁾The difference between the even and odd orders of multiphonon scattering was apparently first noted by Genkin.^[13] The conclusion he drew, however, that the odd-order scattering process have a dipole-forbidden character, seems to be in error.

⁴⁾J. F. Scott, R. C. C. Leite, and T. C. Damen, Phys. Rev. **188**, 1285 (1969).

²⁾E. Gross, S. Permogorov, Ya. Morozenko, and B. Kharlamov, Phys. Status Solidi **B59**, 551 (1973).

³⁾V. M. Genkin, Zh. Eksp. Teor. Fiz. **58**, 2005 (1970) [Sov. Phys. JETP **31**, 1080 (1970)].

⁴⁾E. Mulazzi, Phys. Rev. Lett. **25**, 228 (1970).

⁵⁾R. Zeyher, Solid State Commun. **16**, 49 (1975).

⁶⁾S. Permogorov, Phys. Status Solidi [B] **68**, 9 (1975).

⁷⁾A. A. Abdumalikov, A. A. Klochikhin, and Yu. M. Shabel'skii, Pis'ma Zh. Eksp. Teor. Fiz. **23**, 444 (1976) [JETP Lett. **23**, 402 (1976)].

⁸⁾A. A. Klochikhin, S. A. Permogorov, and A. N. Reznitskii, Fiz. Tverd. Tela (Leningrad) **18**, No. 8 (1976) [Sov. Phys. Solid State **18**, No. 8 (1976)].

⁹⁾A. A. Abrikosov, L. P. Gor'kov, and I. E. Dzyaloshinskii, Metody kvantovoi teorii polya v statisticheskoi fizike (Quantum Field Theoretical Methods in Statistical Physics), Fizmatgiz, 1962, Chaps. 2, 3. [Pergamon, 1965].

¹⁰⁾D. S. Bulyantisa and A. A. Klochikhin, Fiz. Tverd. Tela (Leningrad) **18**, 458 (1976) [Sov. Phys. Solid State **18**, 265 (1976)].

¹¹⁾R. F. Kazarinov and O. V. Konstantinov, Zh. Eksp. Teor. Fiz. **40**, 936 (1961) [Sov. Phys. JETP **13**, 654 (1961)].

¹²⁾R. M. Martin, Phys. Rev. **B4**, 3676 (1971).

¹³⁾R. Zeyher, C. S. Ting, and J. L. Birman, Phys. Rev. **B10**, 1725 (1974).

¹⁴⁾S. I. Pekar, Usp. Fiz. Nauk **50**, 197 (1953).

¹⁵⁾S. A. Permogorov, V. V. Travnikov, and A. V. Sel'kin, Fiz. Tverd. Tela (Leningrad) **14**, 3642 (1972) [Sov. Phys. Solid State **14**, 3051 (1973)].

¹⁶⁾S. Permogorov and A. Reznitsky, Solid State Commun. **18** (1976).

¹⁷⁾M. A. Nusimovici and J. L. Birman, Phys. Rev. **156**, 925 (1967).

¹⁸⁾E. F. Gross, S. A. Permogorov, and B. S. Razbirin, Fiz. Tverd. Tela (Leningrad) **8**, 1483 (1966) [Sov. Phys. Solid State **8**, 1180 (1967)].

¹⁹⁾S. A. Permogorov, Ya. V. Morozenko, and B. A. Kazennov, Fiz. Tverd. Tela (Leningrad) **17**, 2970 (1975) [Sov. Phys. Solid State **17**, 1974 (1975)].

²⁰⁾A. A. Klochikhin and A. G. Plyukhin, Pis'ma Zh. Eksp. Teor. Fiz. **21**, 267 (1975) [JETP Lett. **21**, 122 (1975)].

²¹⁾S. A. Permogorov, A. N. Reznitskii, Ya. V. Morozenko, and B. A. Kazennov, Fiz. Tverd. Tela (Leningrad) **16**, 2403 (1974) [Sov. Phys. Solid State **16**, 1562 (1975)].

²²⁾Y. A. Abramov, S. Permogorov, B. S. Razbirin, and A. J. Ekimov, Phys. Status Solidi **42**, 627 (1970).

²³⁾S. A. Permogorov and V. V. Travnikov, Fiz. Tverd. Tela (Leningrad) **13**, 709 (1971) [Sov. Phys. Solid State **13**, 586 (1971)].

²⁴⁾P. Wiesner and U. Heim, Phys. Rev. **B11**, 3071 (1975).

²⁵⁾E. Gross, S. A. Permogorov, V. Travnikov, and A. Selkin, Solid State Commun. **10**, 1071 (1972).

²⁶⁾V. A. Kiselev, B. S. Razbirin, and J. N. Uraltsev, Phys. Status Solidi **B72**, 161 (1975).

Translated by J. G. Adashko